Dalton Transactions



COMMUNICATION

View Article Online



Cite this: *Dalton Trans.*, 2019, **48**, 2872

Received 23rd January 2019, Accepted 24th January 2019 DOI: 10.1039/c9dt00324j

rsc.li/dalton

Hard *versus* soft: zero-field dinuclear Dy(III) oxygen bridged SMM and theoretical predictions of the sulfur and selenium analogues†

Kuduva R. Vignesh, Dimitris I. Alexandropoulos, Brian S. Dolinar And Kim R. Dunbar **

Two dinuclear lanthanide complexes (Gd and Dy) were prepared and characterized by X-ray, magnetic and computational methods. The Dy analogue shows SMM behavior with an energy barrier of 98.4 K in the absence of an applied dc field. Theoretical calculations were performed on model complexes which support the hypothesis that the energy barrier will increase if the soft-donor atoms S and Se are used in lieu of an O donor.

Single Molecule Magnets (SMMs)¹ are prominent members of coordination chemistry field, owing to their promising potential applications in information storage devices,² Q-bits³ and in spintronic devices.3a,4 SMMs are mononuclear or polynuclear transition, rare earth or mixed d/f metal complexes that exhibit slow relaxation of the magnetization, and act as nano-magnets below a certain blocking temperature. The electronic structure of the metal ions, magnetic anisotropy and magnetic exchange interactions constitute the fundamental ingredients for the existence of a barrier and quantum tunnelling, which lead to bistability and slow paramagnetic relaxation in SMMs.5 Since the discovery of slow relaxation of magnetization in single-ion lanthanide complexes,6 tremendous progress in the synthesis and study of lanthanide based SMMs.⁷ The inherent magnetic anisotropy and the number of unpaired f-electrons are responsible for the high energy barrier for the reversal of magnetization in Ln SMMs.8 Importantly, Dy^{III} is the most promising candidate, ^{8d} with Dy^{III} organometallic molecules exhibiting blocking temperatures of 60 K and 80 K having been reported. Research has also focused on the 4f-ion based polynuclear clusters8a-c and their combination with transition metals {3d-4f} or radicals {2p-4f}. The observed SMM characteristics of these complexes

Department of Chemistry, Texas A&M University, College Station, Texas 77842-3012, USA. E-mail: dunbar@chem.tamu.edu

†Electronic supplementary information (ESI) available: Synthetic, crystallographic, computational, and magnetic details. CCDC 1880175 and 1880176. For ESI and crystallographic data in CIF or other electronic format see DOI: 10.1039/c9dt00324j

can be ascribed to the single ion anisotropy of Dy^{III} ions, but a primary challenge in such clusters is the very weak exchange interaction leading to the existence of low-lying excited states, the population of which leads fast quantum tunnelling of the magnetization (QTM).8a,11 Although there have been considerable efforts to elucidate the mechanisms operative for mononuclear 4f SMMs, much less attention has been devoted in understanding the relaxation mechanisms in polynuclear 4f SMMs. The primary hurdle is to assess the impact of the Ln...Ln exchange interaction on the SMM property where the individual single-ion anisotropies are assumed to be the dominant phenomenon. The choice of the bridging group is important to overcome the core nature of the 4f orbitals and subsequently induce significant exchange interaction between the paramagnetic centres. Moreover, the ligand field as well as the coordination geometry exert a strong influence on the local anisotropy of the lanthanide ion. To put it in simple terms, the SMM behaviour is governed by the interplay between the ligand field effect, the geometry, and the strength of the magnetic exchange interaction between the lanthanide ions. Notably, a study on a $[Dy_2(ovph)_2Cl_2(MeOH)_3]$ (where $H_2ovph =$ pyridine-2-carboxylic acid [(2-hydroxy-3-methoxyphenyl) methylene] hydrazide) dinuclear complex by Powell et al. 12 has shown that Ising type exchange interactions between the DyIII ions suppresses the QTM at zero field and shows the importance of exchange interactions in developing next generation SMMs. Also, the work of Murray et al. 13 on {Co₂^{III}Dy₂} butterfly complexes and their ab initio calculations suggest that the exchange interaction between DyIII ions can be improved to suppress the QTM by utilising diamagnetic 3d ions adjacent to the Dy^{III} centres.

With the aforementioned issues as a backdrop, herein we report the synthesis, structures, magnetic, and theoretical studies of two new homodinuclear lanthanide(III) complexes, $[HNEt_3]_x[Ln_2^{III}(LH_4)_2(dbm)_2](NO_3)_y$ (Ln = Gd, x = 1, y = 3 for (1), and Ln = Dy, x = 0, y = 2 for (2), where LH_4^- = singly deprotonated 2,2-bis(hydroxymethyl)-2,2',2"-nitrilotriethanol, dbm = 1,3-diphenyl-1,3-propanedionate) (Scheme 1). The principal

Dalton Transactions Communication

Scheme 1 Synthetic route employed for the synthesis of 1 and 2.

aim is to fully understand the electronic structure, quantify the magnetic anisotropy, investigate the magnetic exchange between the lanthanide centres and, finally, to predict how to improve the relevant parameters that contribute to an increase in the magnetisation reversal barrier by replacing the O-donor bridging atoms with the softer donor atoms S and Se.

Reactions of Ln(NO₃)₃·xH₂O (Ln = Gd^{III} and Dy^{III}), dbmH and LH₅ in a 1:2:1 molar ratio with triethylamine (Et₃N) solution in MeCN produce pale yellow crystals of [HNEt3][Ln2III] $(LH_4)_2(dbm)_2(NO_3)_3$ (1) and $[Dy_2(LH_4)_2(dbm)_2(NO_3)_2$ (2). The chemical and structural identities of the compounds were confirmed by single-crystal X-ray crystallography (Table S1†), elemental analyses (C, H, N), and IR spectral data (ESI†).

Due to the structural similarities of complexes 1 and 2, only complex 2 will be described as a representative example. Complex 2 crystallizes in the triclinic space group $P\bar{1}$ and its asymmetric unit consists of one half of the [Dy₂(LH₄)₂(dbm)₂]²⁺ cation and a nitrate anion, with the remainder related through a crystallographic centre of inversion. A labelled representation of the cation of 2 is presented in Fig. 1 and consists of two Dy atoms doubly bridged by deprotonated alkoxido arms of two η¹:η¹:η¹:η¹:η²:μ LH₄ moieties and act as tetradentate N/O-chelates and O-bridging ligands. The resulting $\{Dy_2(\mu-OR)_2\}^{4+}$ core is nearly planar with the Dy1...Dy1' axis (3.743(2) Å) with a Dy1-O1-Dy1' angle of 110.67(2)°. The Dy-O/N bond distances are slightly shorter than the corresponding Gd-O/N ones due to the lanthanide contraction. The eight-coordinate Dy ions are completed by the O atoms of two chelating dbm- ligands. The coordination geometry of the Dy ions can be best described as triangular dodecahedral, based on SHAPE¹⁴ calculations (Table S2†).

The unit cell of 2 also contains two NO₃⁻ ions which are involved in strong intermolecular hydrogen bonding with the

Fig. 1 (Left) Structure of the cation of 2 and (right) triangular dodecahedral geometry of Dy1 in the structure of 2. H atoms were omitted for the sake of clarity. Colour scheme: Dy, yellow; N, blue; O, red; C, black.

protonated (R-OH) arms of the LH₄⁻ ligands (this includes the O atoms of the LH₄⁻ ligand, O2, O4, and O5, as the donors, and the nitrate O atoms, O8, and O9, as the acceptors) (ESI†). In addition, there are some weak hydrogen bonding contacts between the protonated (R-OH) arms of the LH₄ ligands and the lattice MeCN molecules (Fig. S1†). The closest intermolecular Dy...Dy contact is 8.070(2) Å. Complex 1 crystallizes in the monoclinic $P2_1/c$ space group, where the [Gd₂(LH₄)₂(dbm)₂]²⁺ cation co-crystallizes with one HNEt⁺ and three NO₃ ions.

The magnetic properties of the two compounds were investigated by direct current (dc) magnetic susceptibility measurements. The $\chi_{M}T$ vs. T plots for 1 and 2 (Fig. 2) reveal room temperature values of 15.15 cm³ K mol⁻¹ and 28.35 cm³ K mol⁻¹ which are in good agreement with the expected values of 15.75 cm³ K mol⁻¹ and 28.34 cm³ K mol⁻¹ for two non-interacting Gd^{III} (${}^8S_{7/2}$, S=7/2, L=0, g=2) and Dy^{III} (${}^{6}H_{15/2}$, S = 5/2, L = 5, g = 4/3) ions, respectively. The $\chi_{M}T$ vs. T plots are similar at temperatures between 300-15 K; the $\chi_{\rm M}T$ values decrease as the temperature is lowered due to depopulation of the Starks sub-levels as a result of single ion crystal-field effects. These results are further supported by the magnitude of the magnetization and the saturation values (Fig. S2†).

The magnetic exchange interaction between the Gd^{III} ions in 1 were extracted by fitting the susceptibility data (Fig. 2) using the PHI program, 15 yielding a weak antiferromagnetic interaction of -0.1 cm $^{-1}$. DFT calculations (see computational details in ESI†) were carried out to compute the magnetic interactions between the GdIII ions, the results of which predict a value of -0.14 cm⁻¹, in good agreement with the experimental value.

In order to probe the SMM properties of 2, frequency dependent out-of-phase magnetic susceptibility and Cole-Cole measurements for 2 were performed using a 2 Oe oscillating ac field at frequencies from 0.1-1000 Hz between 1.8 and 14 K, under a zero static de field. Evidence of SMM behaviour is observed for 2 (Dy) with χ''_{M} versus frequency plots displaying out-of-phase susceptibility maxima (Fig. 3, top). Cole-Cole plots of χ'_{M} versus χ''_{M} data exhibit semi-circular profiles which

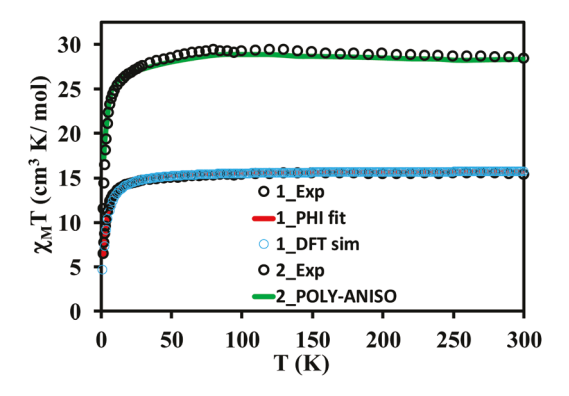


Fig. 2 Variable-temperature dc magnetic susceptibility data for 1 and 2, under an applied field of 0.1 T.

Dalton Transactions Communication

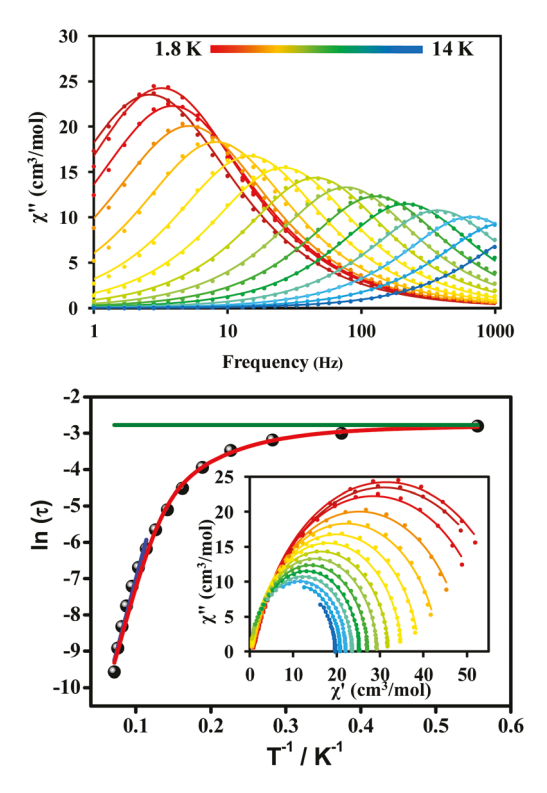


Fig. 3 (Top) Frequency dependence of $\chi^{\prime\prime}_{\ M}$ for 2 in a zero applied dc field, with an ac magnetic field of 2 Oe. (Bottom) Magnetization relaxation time (τ) , plotted as $\ln \tau$ vs. T^{-1} for 2. The solid blue line corresponds to fitting of the Orbach relaxation process, and the solid red line represents the fitting to multiple relaxation processes. The horizontal green line represents the QTM relaxation time. (Inset) Cole-Cole plots between 1.8 and 14 K. The colour lines are fitted data extracted from CC-FIT program.17

indicate a single relaxation process for 2 (Fig. 3, bottom inset). Plots of $ln(\tau)$ versus 1/T are linear (Fig. 3, bottom) between 10.5-14 K, indicating that a thermally activated Orbach process is operative. The data were fit (Table S3†) considering all the possible relaxation processes using the equation, $1/\tau =$ $1/\tau_{\rm OTM} + CT^n + \tau_0^{-1} \exp(U_{\rm eff}/k_{\rm B}T)$, where $1/\tau_{\rm OTM}$ corresponds to the relaxation process via quantum tunnelling pathway, the CTⁿ term corresponds to the relaxation via Raman process, and the last term accounts for the Orbach relaxation pathway.¹³ The values obtained from the best fit are n = 3.5(2), $C = 0.11(4) \text{ s}^{-1} \text{ K}^{-3.5}, U_{\text{eff}} = 98.4(8) \text{ K and } \tau_0 = 3.7(1) \times 10^{-5} \text{ s}$ (R = 0.997) for 2. The *n* value is lower than expected and this can be attributed to the presence of both optical and acoustic Raman processes involving magnetic relaxation. 16 A QTM relaxation time, $\tau_{\rm OTM}$, of 0.06 s is estimated and a convincing pre-exponential factor (10^{-5} s) allows confidence in the extracted values for an SMM.8d

To understand the single ion relaxation process, we performed CASSCF + RASSI-SO calculations to compute the anisotropy of both DyIII ions in 2 (see Computational details in ESI†). In both Dy^{III} ions, $m_I = \pm 15/2$ states were found to be stabilized as the ground state. Moreover, the g_z values were almost purely axial in nature with negligible transverse

 $(g_x = 0.0044, g_y = 0.0072, \text{ and } g_z = 19.696 \text{ for Dy ions})$ components (Table S4†). Thus, the mixing of the $m_I = \pm 15/2$ states with other m_I states was significantly reduced due to the increased energy gap between the ground and the first excited Kramers doublet (KD). The energy gaps were found to be 158.0 cm⁻¹ for both Dy ions (Table S5†), indicating that they are symmetrically equivalent. Since the first excited KD is significantly higher in energy, this suggests a possibility for the magnetization blockade at the single ion level.

To determine the relaxation processes associated with the single ion anisotropy of DyIII ions, the relaxation mechanisms were developed and are shown in Fig. 4. In both Dy ions in 2, the ground state QTM probability is small $(0.2 \times 10^{-2} \mu_{\rm B})$ due to the dominance of axial crystal field parameters (Table S6†) and the first excited state TA-QTM (Temperature Assisted QTM) probability is significantly large. 13 This suggests that the magnetic relaxation occurs via the first excited state with an energy barrier of 158 cm⁻¹ (227.3 K). The anisotropy barrier of 2 was then computed considering the exchange coupled states of both DyIII ions using the POLY_ANISO program. 18 The magnetic susceptibility data were used to extract the DyIII...DyIII exchange coupling, yielding a value of -0.01 cm^{-1} (see Fig. 2). Although weak antiferromagnetic exchange introduces several low-lying states, the relaxation occurs via second excited states, due to the tunnelling of the magnetization (Table S7 and Fig. S4†). The coupled state anisotropy barrier, $U_{\text{cal}} =$ 158.2 cm⁻¹ (227.6 K) is relatively large as compared to the experimentally determined barrier of 98.4 K.

It is well known that structural parameters can profoundly affect the magnetic behaviour of a particular complex, especially through the bridging atoms. These considerations include structural modifications of donor atoms such as S and Se lieu of O atom. This strategy has been successfully achieved to increase the magnetic coupling constants and the zero-field splitting parameter (D) in transition metal complexes, 19 but

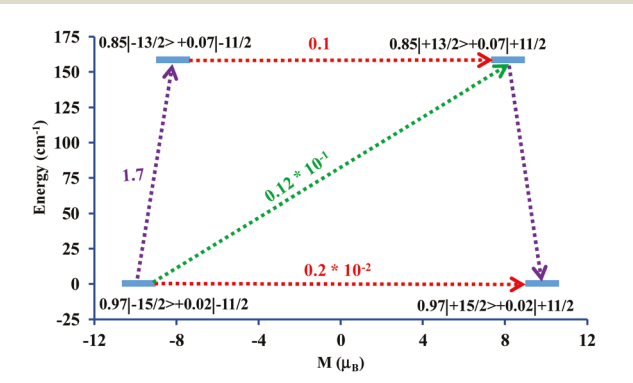


Fig. 4 The ab initio computed magnetization blocking barrier for Dy1 site in 2. The thick blue line indicates the KDs as a function of the computed magnetic moment. The green/purple dotted arrows show the possible pathway through the Orbach/Raman relaxation. The red dotted arrows represent the presence of QTM and TA-QTM between the connecting pairs. The numbers provided at each arrow are the mean absolute value for the corresponding matrix element of the transition mag-

Dalton Transactions Communication

this strategy has not been widely utilised in lanthanide coordination complexes although some organometallic compounds exhibit improved SMM properties.²⁰ In this vein, we postulated that it would be interesting to model two complexes by replacing the bridging O-atoms with S and Se atoms in 2. The model complexes 2-S and 2-Se were optimised using DFT calculations (Fig. S3†) and the optimised structures were used to study the magnetic behaviour using ab initio calculations.

The single-ion calculations performed for 2-S and 2-Se on both DyIII ions suggest that the local g-tensors in the ground KD are purely axial in nature, with very small transverse components $(g_x = 0.0027, g_y = 0.0037, \text{ and } g_z = 19.7358 \text{ for Dy1 of}$ **2-S** and $g_x = 0.0017$, $g_y = 0.0020$, and $g_z = 19.7847$ for Dy1 of 2-Se). The presence of soft-donor atoms yields even smaller transverse terms compared to those for 2. A small TA-QTM in the first excited state $(0.6 \times 10^{-1} \mu_{\rm B} \text{ for Dy1 of 2-S and } 0.4 \times$ $10^{-1}\mu_{\rm B}$ for Dy1 of 2-Se) allows the magnetization to relax via the second excited state and the energy barriers were found to be 192.7 cm⁻¹ (Dy1) and 201.9 cm⁻¹ (Dy2) in 2-S, 315.3 cm⁻¹ (Dy1) and 353.3 cm⁻¹ (Dy2) in 2-Se (Table S5†). These values are larger than that observed for complex 2, owing to a stronger electrostatic interaction afforded by the soft-donor atoms. A qualitative mechanism for the magnetic relaxation for the Dy1 sites in 2-S and 2-Se obtained from the ab initio calculations is shown in Fig. 5. The coupled states barriers were extracted with a DyIII...DyIII exchange of -0.05 and -0.07 cm-1 for 2-S and 2-Se, respectively using POLY_ANISO. The improved magnetic couplings predict a smaller tunnelling probability in the ground state $(1.5 \times 10^{-7} \text{ cm}^{-1} \text{ for } 2\text{-S} \text{ and})$ 3.7×10^{-8} cm⁻¹ for 2-Se). Furthermore, it was found that the tunnelling probability is very small until the 9th and 10th

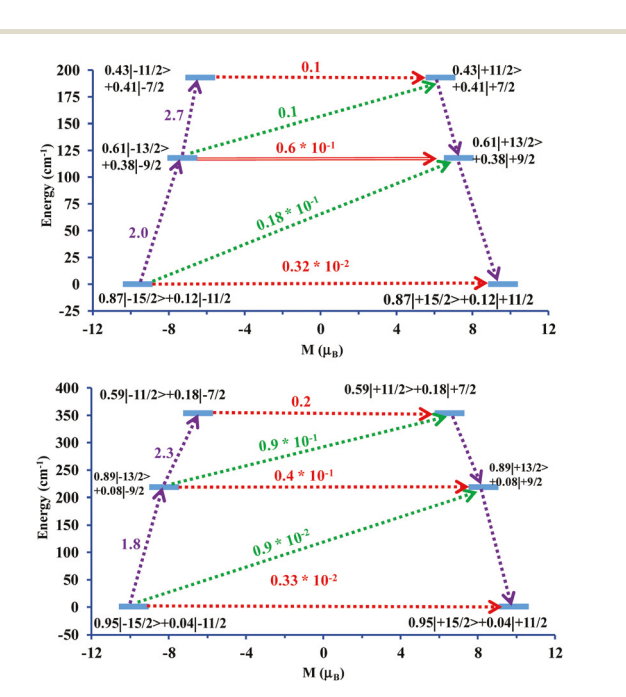


Fig. 5 The ab initio computed magnetization blocking barrier for the Dy1 sites in (top) 2-S, (bottom) 2-Se.

excited states and the magnetic relaxation proceeds to the 10th and 11th excited states (Tables S8 and S9†) for 2-S and 2-Se, respectively. Thus, these calculations show that the DyIII...DyIII exchange suppresses the tunnelling for both complexes, in comparison to the single ion, leading to a barrier height of 239.8 and 419.8 cm⁻¹ for 2-S and 2-Se, respectively. These $U_{\rm cal}$ are larger than that computed for complex 2 (158.2 cm⁻¹), suggesting that there is an advantage in using soft-donors in place of hard-donor atoms.

Structural, magnetic and ab initio CASSCF studies were used to quantify the observed magnetic behaviour of two lanthanide dinuclear complexes. The effect of soft-donor atoms was probed using theory in order to ascertain the effect of magnetic anisotropy combined with magnetic coupling of the individual Dy ions in the dinuclear SMMs. These combined experimental and computational analyses serve as a benchmark for the theoretical model, which can be used for the design and optimization of lanthanide-based SMMs. Work is in progress to synthesize polynuclear 4f complexes with softdonor atoms.

Conflicts of interest

There are no conflicts to declare.

Acknowledgements

We thank the National Science Foundation (CHE- 1808779) and Welch Foundation (A-1449) for support. We are grateful to the HPRC at Texas A&M for the computing resources.

Notes and references

- 1 (a) R. Sessoli, D. Gatteschi, A. Caneschi and M. A. Novak, Nature, 1993, 365, 141-143; (b) G. Christou, D. Gatteschi, D. N. Hendrickson and R. Sessoli, MRS Bull., 2000, 25, 66-71.
- 2 (a) D. Gatteschi, R. Sessoli and J. Villain, Molecular Nanomagnets, Oxford University Press, Oxford, 2006; (b) D. Gatteschi, Adv. Mater., 1994, 6, 635-645.
- 3 (a) E. Coronado and A. J. Epstein, J. Mater. Chem., 2009, 19, 1670-1671; (b) M. N. Leuenberger and D. Loss, Nature, 2001, 410, 789-793.
- 4 L. Bogani and W. Wernsdorfer, Nat. Mater., 2008, 7, 179-186.
- 5 (a) M. Atanasov, P. Comba, S. Hausberg and B. Martin, Coord. Chem. Rev., 2009, 253, 2306-2314; (b) F. Neese and D. A. Pantazis, Faraday Discuss., 2011, 148, 229-238.
- 6 (a) N. Ishikawa, M. Sugita, T. Ishikawa, S. Koshihara and Y. Kaizu, J. Am. Chem. Soc., 2003, 125, 8694-8695; (b) N. Ishikawa, M. Sugita and W. Wernsdorfer, Angew. Chem., Int. Ed., 2005, 44, 2931-2935; (c) N. Ishikawa, M. Sugita, T. Ishikawa, S. Koshihara and Y. Kaizu, J. Phys. Chem. B, 2004, 108, 11265-11271.

7 (a) Y.-C. Chen, J.-L. Liu, W. Wernsdorfer, D. Liu, L. F. Chibotaru, X.-M. Chen and M.-L. Tong, *Angew. Chem., Int. Ed.*, 2017, 56, 4996–5000; (b) C. A. P. Goodwin, F. Ortu, D. Reta, N. F. Chilton and D. P. Mills, *Nature*, 2017, 548, 439–442; (c) S. K. Gupta, T. Rajeshkumar, G. Rajaraman and R. Murugavel, *Chem. Sci.*, 2016, 7, 5181–5191; (d) F.-S. Guo, B. M. Day, Y.-C. Chen, M.-L. Tong, A. Mansikkamäki and R. A. Layfield, *Angew. Chem., Int. Ed.*, 2017, 56, 11445–11449.

Communication

- 8 (a) R. J. Blagg, C. A. Muryn, E. J. L. McInnes, F. Tuna and R. E. P. Winpenny, Angew. Chem., Int. Ed., 2011, 50, 6530–6533; (b) S. K. Langley, N. F. Chilton, I. A. Gass, B. Moubaraki and K. S. Murray, Dalton Trans., 2011, 40, 12656–12659; (c) S. K. Langley, B. Moubaraki, C. M. Forsyth, I. A. Gass and K. S. Murray, Dalton Trans., 2010, 39, 1705–1708; (d) R. Sessoli and A. K. Powell, Coord. Chem. Rev., 2009, 253, 2328–2341.
- 9 F.-S. Guo, B. M. Day, Y.-C. Chen, M.-L. Tong, A. Mansikkamäki and R. A. Layfield, *Science*, 2018, 362(6421), 1400–1403.
- (a) T. Rajeshkumar and G. Rajaraman, Chem. Commun.,
 2012, 48, 7856–7858; (b) M. K. Singh, N. Yadav and G. Rajaraman, Chem. Commun., 2015, 51, 17732–17735;
 (c) J. D. Rinehart, M. Fang, W. J. Evans and J. R. Long, J. Am. Chem. Soc., 2011, 133, 14236–14239;
 (d) J. D. Rinehart, M. Fang, W. J. Evans and J. R. Long, Nat. Chem., 2011, 3, 538–542; (e) B. S. Dolinar, D. I. Alexandropoulos, K. R. Vignesh and K. R. Dunbar, J. Am. Chem. Soc., 2018, 140, 908–911.

- L. Ungur, S. K. Langley, T. N. Hooper, B. Moubaraki,
 E. K. Brechin, K. S. Murray and L. F. Chibotaru, *J. Am. Chem. Soc.*, 2012, 134, 18554–18557.
- 12 Y.-N. Guo, G.-F. Xu, W. Wernsdorfer, L. Ungur, Y. Guo, J. Tang, H.-J. Zhang, L. F. Chibotaru and A. K. Powell, *J. Am. Chem. Soc.*, 2011, 133, 11948–11951.
- 13 K. R. Vignesh, S. K. Langley, K. S. Murray and G. Rajaraman, *Inorg. Chem.*, 2017, **56**, 2518–2532.
- 14 S. Alvarez, P. Alemany, D. Casanova, J. Cirera, M. Llunell and D. Avnir, *Coord. Chem. Rev.*, 2005, 249, 1693–1708.
- N. F. Chilton, R. P. Anderson, L. D. Turner, A. Soncini and K. S. Murray, J. Comput. Chem., 2013, 34, 1164–1175.
- 16 K. N. Shrivastava, *Phys. Status Solidi B*, 1983, **117**, 437–458.
- 17 N. F. Chilton, *CC-fit*, The University of Manchester, UK, 2014, http://www.nfchilton.com/cc-fit.html.
- 18 L. F. Chibotaru and L. Ungur, *POLY_ANISO program*, University of Leuven, 2006.
- (a) L. Fohlmeister, K. R. Vignesh, F. Winter, B. Moubaraki,
 G. Rajaraman, R. Pöttgen, K. S. Murray and C. Jones,
 Dalton Trans., 2015, 44, 1700–1708; (b) S. Vaidya,
 A. Upadhyay, S. K. Singh, T. Gupta, S. Tewary, S. K. Langley,
 J. P. S. Walsh, K. S. Murray, G. Rajaraman and
 M. Shanmugam, Chem. Commun., 2015, 51, 3739–3742.
- 20 (a) T. Pugh, V. Vieru, L. F. Chibotaru and R. A. Layfield, Chem. Sci., 2016, 7, 2128–2137; (b) F. Tuna, C. A. Smith, M. Bodensteiner, L. Ungur, L. F. Chibotaru, E. J. L. McInnes, R. E. P. Winpenny, D. Collison and R. A. Layfield, Angew. Chem., Int. Ed., 2012, 51, 6976–6980.